Geoinformation for European-wide Integration, Benes (ed.)

Integration of remote sensing and GIS for groundwater assessment in Eritrea

S. Solomon & F. Quiel
Environmental and Natural Resources Information Systems, Royal Institute of Technology, Stockholm, Sweden
semere@kth.se , friedrich.quiel@byv.kth.se

Keywords: remote sensing, GIS, hard rock, groundwater, lithology, lineament, Eritrea

ABSTRACT: An integrated approach with remote sensing, GIS and traditional fieldwork techniques was adopted to assess the groundwater potential in the central highlands of Eritrea. Digitally enhanced color composites and panchromatic images of Landsat TM and Spot were interpreted and thematic maps on lithology and lineaments prepared. Structural features were measured in the field and orientations compared with lineaments derived from both remote sensing data and a DEM. Hydrogeological setting of selected springs and wells were investigated in field excursion, from well logs and pumping test data. All thematic layers were integrated and analysed in a GIS. Results show that high yielding wells and springs are often related to large lineaments and corresponding structural features. Fractures in hydraulic connection with alluvium and weathered bedrock constitute best aquifers. The results demonstrate that the integration of remote sensing, GIS and traditional fieldwork provide a powerful tool in the assessment of water resources.

1 INTRODUCTION

The use of satellite borne remote sensing data has proved to be an effective data source to facilitate the preparation of lithological and structural maps. At a regional scale, these data can display major rock groups, structural features, such as folds, faults, lineament, and fracture, due to their synoptic coverage and multispectral capability (e.g. Sabins 1978, Drury 1987). Remote sensing images can visually be interpreted in an efficient and effective way using several basic interpretation keys or elements (Sabins, 1978). Similarly a number of procedures are available for image data manipulation (Jensen 1986, Lillesand and Kiefer 1994, Drury 1987).

The full potential of remote sensing and GIS can be utilized when an integrated approach is adopted. Integration of the two technologies has proven to be an efficient tool in groundwater studies (Krishnamurthy et. al 1996, Sander 1996, Saraf and Choudhury 1998). Groundwater in hard rock aquifers is essentially confined to fractured and weathered horizons. Therefore, an extensive hydrogeological investigation is required to thoroughly understand groundwater conditions. Remote sensing data provide accurate spatial information and can be economically utilized over conventional methods of hydrogeological surveys. Digital enhancement of satellite data support extraction of maximum information due to increased interpretability. GIS techniques facilitate integration and analysis of large volumes of data. Field studies help to validate results further. Integrating all these approaches provides better understanding of groundwater controlling features in hard rock aquifers.

Eritrea is located in the horn of Africa and is geographically bounded by Ethiopia to the south, Sudan to the west and north, the Red Sea to the east and Djibouti to the southeast (figure 1). The country is divided into three physiographic regions, namely: the western lowlands (500 – 1500 m), central highlands (1500 – 2500 m) and eastern coastal lowlands (0 – 1500 m). The climate is arid to semi-arid and there are two rainy seasons in the study area. The long rainy season during the summer is from June to September, and the short spring rain during March to April. Rainfall is intense during the periods mid-July to mid–August. Average annual precipitation is from 300 to 600 mm. Potential evapotranspiration is approximately 1700 mm/yr. Daily temperatures usually vary from 10^{o} to 30^{o} C.

Eritrea is part of the Arabian-Nubian Shield and is characterized by a low-grade volcanosedimentary-ophiolite assemblage, granitoids and gneisses (e.g. Vail, 1987). The Precambrian terrain of Eritrea forms the least studied portion of the Arabian-Nubian Shield. Several classifications have been proposed for the Precambrian rocks of Eritrea (e.g.

Drury and Berhe 1993, Ghebreab 1996). The regional geology of the central highlands where this study is focused is given in figure 1. The crystalline rocks (hard rocks) are comprised of granitoids and metamorphic rocks which cover most of the region. The sandstone unit (Mesozoic) and basaltic flows (Cenozoic) lie unconformably over the crystalline rocks.

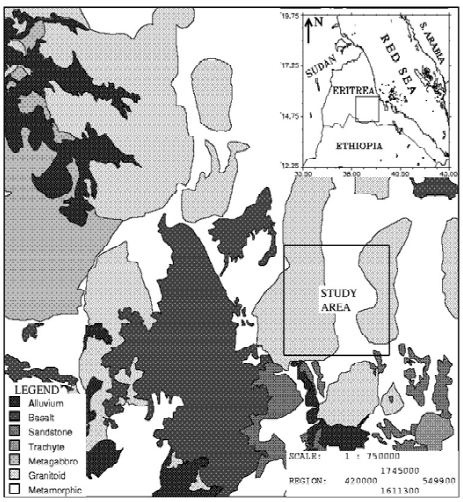

Figure 1. Location and regional geologic map.

A test site of 30 x 30 km was mapped to identify the major lithologies and structures. The main objective of the present study is thus to assess groundwater controlling features in this part of the country. ENVI (the Environment for Visualizing Images) version 3.5 and GRASS (Geographical Resources Analysis Support System) version 4.3/5.0 software packages were used for image processing and GIS analysis, respectively.

2 METHOD

2.1 *Remote Sensing*

Landsat TM 4 data (path/row 169/050, acquired September 1987, 28.5 m resolution) and Spot 5 Multispectral data (row/column 136/320, acquired April 1996, 20m resolution) were used for lithological and lineament mapping. Subscenes of 30 x 30 km in size were created from both the TM and SPOT images to match the study area. For lineament mapping, a digital elevation model (DEM) with 50 m resolution was used in addition to the remote sensing data. The raw image data were geometrically and radiometrically corrected. The Universal Transverse Mercator (UTM) coordinate system was used in the map.

Several image processing techniques were applied for lithological mapping. As only three bands are needed for a color composite display, first band selection was performed using determinant analyses (Sheffield 1985). Principal Component Analysis (PCA) was performed for the six reflective TM bands to reduce the dimensionality and increase the information content of TM data. Moreover, the selected band combination (TM 1, 4, 5) was subjected to IHS-transformations (Intensity, Hue and Saturation). After a gaussian stretch was performed on the saturation band, the IHS data are transformed back to the RGB (red, green, blue) color space. Finally, decorrelation stretching (DS) was applied on TM bands 1, 4 and 5 to remove the high correlation commonly found in the multispectral data sets and to accentuate the colors in the composite image. A lithological map was then interpreted from all the digital outputs supported by ground truth data and entered into a GIS.

Lineament interpretation is based on visual interpretation of various digitally enhanced single band (TM band 5, SPOT band 3, PC1 and Intensity images) and multi-band composites that involve band combinations, Principal component images, IHS-transformed and decorrelated and stretched images. Also spatial domain filtering was employed on single band images using digital filters for different directions. An array of 3x3 pixel size kernel was selected and applied along directions N-S (0°), NW (315°), NE (45°) and E-W (90°) to highlight the linear features in their respective directions. The lineaments were identified by visual inspections and digitized interactively on the images. Previously interpreted lineaments were restored on and compared with each digitally enhanced image. The lineament mapping was done separately for each of the raw data sets, that is, Landsat TM, SPOT and DEM images. A total lineament map was constructed based on these three inputs and entered into a GIS.

2.2 *Structures*

In the field fracture orientations were obtained by measuring the dip and dip direction with a compass. The data were grouped according to rock type and proximity of sampling points to take into account the geographical locations of observation points. Orientations of all steeply dipping (60°-90°) fracture entries measured have been processed as rose diagrams for each rock type and their orientations compared with the rose diagrams derived from lineaments. Rose diagrams of dykes were constructed and compared with the rose diagrams of joints and lineaments. Photographs of major structures were also collected.

2.3 *Hydrogeology*

The hydrogeological data were entered into a GIS and site maps of water point yields created and converted into raster format. After the integration of the different map layers in a raster based GIS, the relationship of water point yields with the lithology and lineament was assessed by calculating the statistics. When assessing the relationship between water point yield and lineament, buffer zones with 20 m distance interval were created and proximity to lineaments and borehole yields correlated. The correlation studies have been carried out for the boreholes using first the original locational values and then GPS (Global Positioning System)-positioned or surveyed boreholes.

Existing well sites and springs were investigated in the field with regard to location, relation to rock type, siting, topography and structure. Lithological log data at selected water points were constructed and correlated to unravel the subsurface hydrogeological controlling features. Pumping test data were used in relation to the lithological log to understand the nature of the aquifer systems in the study area.

3 RESULTS AND DISCUSSIONS

3.1 *Remote Sensing*

Most of the lithologic units can be recognized in all the processed images; however, certain lithologic features are more enhanced in certain outputs than others. For instance, the post-tectonic granitic intrusion is less defined in the colour composite of TM bands 5, 4 and 1 and PC 1, 2, 3 images (in RGB order). The same feature appears well outlined in the IHS and DS images due to better color saturation. In certain cases, PC 3, 2, 4 was superior in delineating geologic contacts between the foliated and non-foliated metavolcanic rocks than all the other digital outputs. The results of this study demonstrate the need to employ several approaches when using image processing techniques for lithological mapping.

Lineaments which mark geological contacts between different lithologies and structures such as dykes are clearly visible in all the digitally processed color composites. Application of directional filtering in most of the directions on TM band 5, PC1, intensity (both TM and SPOT) images generally highlighted the major lineaments. Off all the directional filters used the N-S oriented were most effective in detecting lineaments (figure 2a), because most of the lineament trends are oblique to the direction of filtering. E-W oriented directional filters were not productive. This is probably due to either the absence of lineaments in this trend or use of small kernel size. It is important to note, however, that certain lineament trends appear more conspicuous on the raw data than the directionally filtered images (figure 2b). This is probably due to tonal variation. Furthermore spatial filtering reduces the gray-level range present in an image (Lillesand and Kiefer, 1994). Application of directional filtering on the PC1 (fig. 2a) and Intensity images enhances the lineaments better than the other single band images. This is probably due to enhancement of topographic features on the PC1 and intensity images.

(a)

(b)

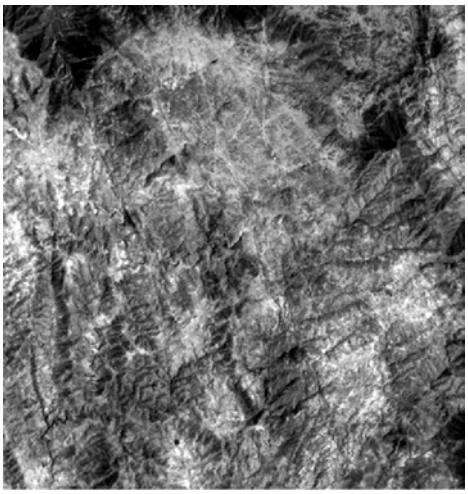

(c)

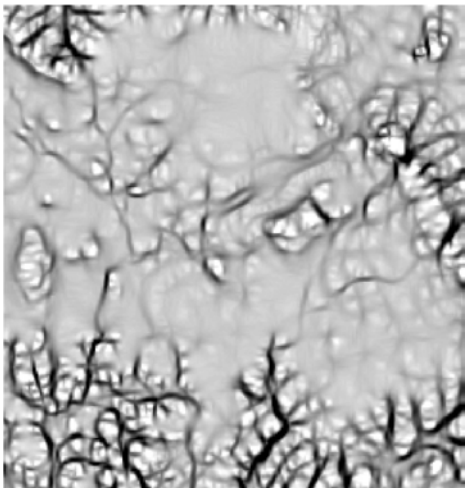

Figure 2. (a) Directional filtering applied along N-S direction on PC1 image (b) Spot band 3 raw image and (c) Topographic model output (minimum curvature) image from DEM.

In the DEM, major lineaments that are mainly expressed by geomorphologic features appear well identified when compared with the remote sensing data (figure 2c). Minor lineaments are discernible in the remote sensing data only. Although all the major linear features are obvious in the DEM data, the density of lineaments is less when compared with the lineaments observed on the Landsat TM and Spot images. This might be attributed to the lower resolution of the DEM (50 m) in comparison to the improved resolution on the TM (30 m) and Spot (20 m) data that offers better spatial resolution to identify lineaments. Figures 3a and 3b are the geological interpretation map of the study area constructed from the inputs of all digitally processed images and the interpreted total lineaments, respectively. Lineament trends are also presented using rose diagram (figure 4). The major trends are N-S, NW-SE, WNW-ESE, NE-SW and ENE-WSW.

3.2 *Structures*

The structural features that are dominant in the study area include fractures (joints and faults), shear foliations and dykes. The orientations of the six steeply dipping joint sets including the number of observations are presented using rose diagrams for the total joint systems in figure 5a. The four most conspicuous ones are oriented NW-SE, NE-SW, N-S and ENE-WSW. These trends are also clearly visible in the rose diagram of lineaments (figure 4) with the N-S oriented being the longest. The least frequent joint sets are oriented NNE-SSW and WNW-ESE.

(a)

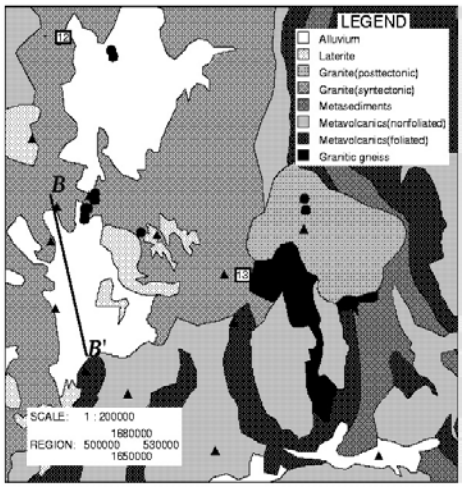

(b)

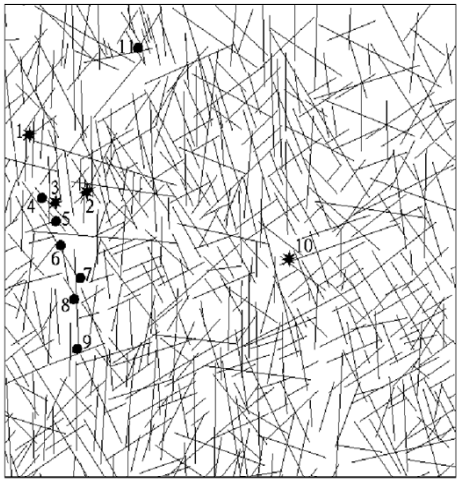

Figure 3 (a) Lithological interpretation map of the study area including locations of joint (triangles) and dyke (circles) measurements and cross-section B-B' in figure 8 (b) Lineament interpretation map showing locations of springs (stars) and wells (circles).

The NNE-SSW trends are only characteristic of the schistose metavolcanic rocks (figure 5b). These joint sets are parallel to the foliation planes and are not observed in the non-foliated metavolcanic (figure 5c), syn-tectonic granites (figure 5d) and post-tectonic granites (figure 5e). The four prominent joint trends are characteristic of most rock units, except in the post-tectonic granites (figure 5e). In this rock unit the nearly perpendicular, NW-SE to NNW-

SSE and ENE-WSW trending joints represent primary joints. Local variations exist between different rock units as well as within a single unit. A minimum of three joint sets is characteristic of most outcrops.

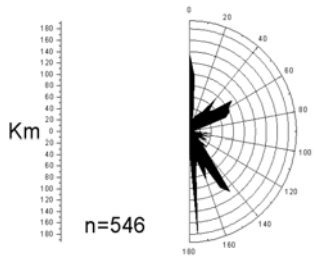

Figure 4. Rose diagram of lineaments with cumulative length in kilometre (km) of lineaments shown on the vertical scale.

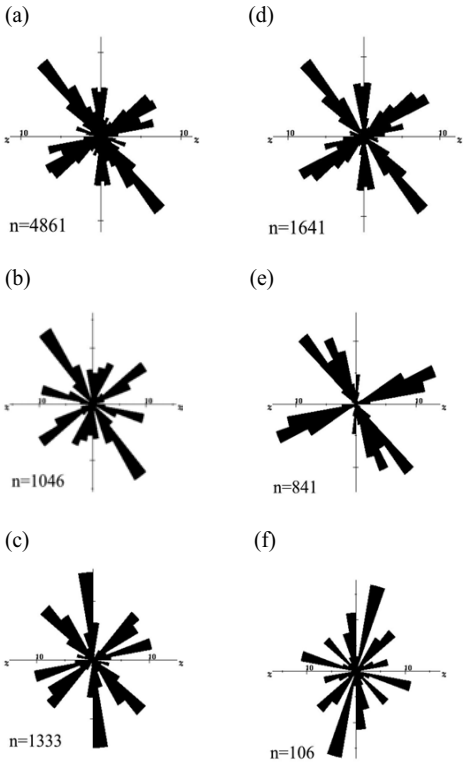

Figure 5. Rose diagrams of (a) total joints (b) schistose metamorphic rocks (c) non-foliated metamorphic rocks (d) syn-tectonic granites (e) post-tectonic granites and (f) dyke swarms.

The dyke swarms in the area (figure 5f) studied exhibit six major trends. The orientations compare well with that of total joints (fig. 5a). However, the most prominent dyke swarms have NNE-SSW trends and compare more to the joint systems in the foliated metamorphic rocks (fig. 5b). This is because these dyke swarms share the strike of the foliation. Most of them are sub-vertically dipping. The dykes are dominantly basaltic to doleritic in composition. All sets of dyke swarms cut the lateritized crystalline basement. Dyke parallel fractures are well developed adjacent to most of the dyke swarms.

Two types of faults, namely normal and strike-slip dominate the study area. The strike-slip faults are oriented generally N-S, WNW-ESE, NE-SW and ENE-WSW, and steeply dipping. Both N-S and NE-SW oriented strike-slip faults have a sinistral sense of movement (e.g. figure 6a, location 12 in fig. 3a). The other two sets, oriented WNW-ESE and ENE-WSW have dextral sense of movement. The normal faults have a number of sets with N-S/NNW-SSE, NW-SE, NE-SW to ENE-WSW strikes that are variable in size and direction and amount of displacement (e.g. figure 6b, location 13 in fig. 3a). Prominent strain markers include Precambrian aplitic dykes/sills. Fault breccias/gouge with associated slickenlines are usually well developed. Most lineaments in the studied area correspond to one of three distinct categories or their associated fractures: (i) dykes; (ii) normal faults (extensional fractures); and (iii) strike-slip faults (shear fractures).

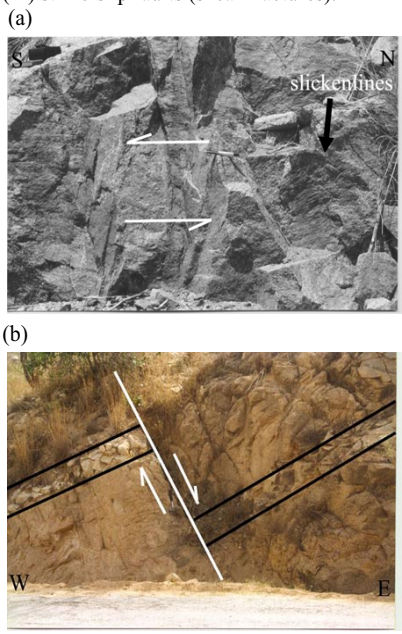

Figure 6. (a) Sinistral N-S trending strike slip-fault showing sub-horizontal structural slickenlines at the contact between the non-foliated metavolcanic and the syn-tectonic granites, location 12 in fig. 3a, and (b) N-S oriented normal fault displacing an aplitic dyke/sill within the syn-tectonic granites, location 13 in fig. 3a.

3.3 *Hydrogeology*

Integration of the hydrogeologic and lithologic data within the GIS show that the log mean yield per unit depth of the saturated thickness is relatively high in the foliated metamorphic rocks with 3.65, followed by granitoids with 3.38 and lowest in the non-foliated metamorphic rocks with 1.73 L/Min/meter. Comparison of the metamorphic rocks show that the schistose variety is more permeable than the massive ones and this is due to the presence of foliation planes that enhance the permeability. The yield varies from one rock type to another as well as within a single type. This shows the inhomogeneous nature of the hard rock aquifers.

Figure 7a shows a comparison between distance to lineaments and logarithmic mean yield of the same borehole population (85), without and with repositioning with GPS. In order to have more data, the analysis is carried out by including data outside the test site. A direct relationship between borehole yield (GPS-positioned) and proximity to satellite image lineaments is shown in figure 7a, while the yield-proximity relationship for boreholes from previous investigations where GPS or surveying have not been used is more ambiguous. Although based on a small borehole population, this study clearly demonstrates the need for accurate coordinates when comparing various spatial data in a geographic information system. Proximity to lineaments does not necessarily imply, however, that the boreholes yield is high. Low yielding boreholes sited on satellite lineaments could occasionally be connected to poorly transmissive dykes or clay gouge in fracture zones (Sander, 1996). The high yielding boreholes seem to have some correlation with the orientation of the lineaments (figure 7b). Although the borehole data available are not sufficient to make a sound correlation, it can be seen that high yielding boreholes are in the proximity of major lineament often with N-S orientations. Most of these lineament trends are related to dykes, normal and strike-slip faults. Field investigations show that siting of some boreholes appears to be guided by proximity to villages and access for drilling rig. This indicates that due considerations are not given to the local structure and/or topography. This may explain the prevalence of low yielding boreholes close to major lineaments.

The borehole geology obtained from the drilling operations are as summarized in the cross-section B-B', figure 8. The results reveal a top alluvial cover of unconsolidated sand to gravel ranging in thickness from 6 to 21 m. The middle lithologic unit is the weathered granitic bedrock, which varies in thickness from 16 to 36 m. At places, 2 - 4 m thick mafic dykes/sills occur within this layer at varying depths. The bottom lithologic unit is the fresh massive bedrock granite and is encountered at varying

(a)

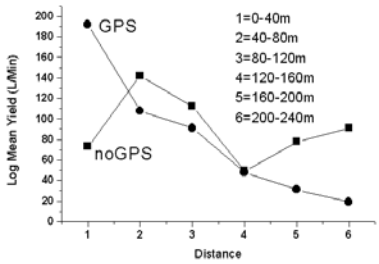

(b)

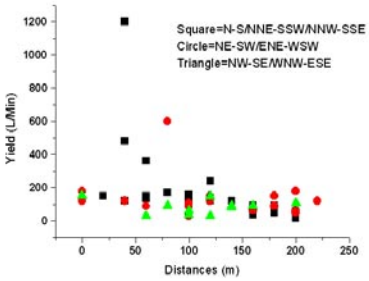

Figure 7. (a) Correlation between borehole log mean yield (Litres per minute) and proximity to lineaments, before and after repositioning with GPS and (b) relation of lineament orientation to borehole yield.

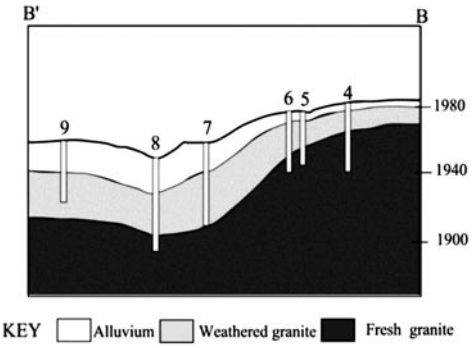

Figure 8. Lithological cross-section along B-B' in the granitic rock aquifers, location fig. 3a.

depths. The water strike depth lies in the top alluvial cover and varies from 8.5 to 14 m at an average borehole yield of about 2 L/s. The estimated yield in the granitic aquifers range from 1.5 to 5.5 L/s. The highest yield is obtained in borehole (8) where the borehole is 60 m deep and the borehole intersects a

dyke at a depth of 41 – 45 m. Moreover this borehole is sited at the intersection of N-S and NW-SE trending lineaments (figure 3b) as well as in a local depression with relatively thick alluvial cover (figure 8). This highlights the significance of structures and local topography when selecting a well site.

The spring at Keih Kor (location 2 in fig. 3a) is flowing along a N-S oriented fracture zone. At Ala (location 11 in fig. 3b) a dug well sunk over NNW-SSE trending dyke yield sustained flow while close by dug wells remain dry. These observations indicate the hydrogeological significance of the lineaments (structures).

A log-log plot of drawdown vs. time for pumping test data is given in figure 9. The response of pumping in the granitic rock aquifers in the two boreholes show consistently an early time-drawdown curve that fits the Theis type curve (radial flow) followed by late time-drawdown curves of linear pattern with very gentle slopes. Depth to static water level in the vicinity of the two boreholes is about 13.5 m and average drawdown is about 4.5 m. The sum of these two (18 m) lies within the weathered horizon. Thus the pumping test results are interpreted as the first segment being due to pumping of water from storage in the weathered zone. The second segment shows more or less constant drawdown due to a contribution from storage in bedrock fractures. Low slopes imply that the fractured bedrock aquifers have low transmissivity. Moreover the variations in drawdown (3 m and 6 m) are attributed to variations in pumping rate (1.39 L/s and 2.81 L/s). Furthermore existence of dry wells sunk in the weathered horizons is reported in the study area. This suggests that the fractured bedrock that is hydraulically connected to the weathered zones controls the occurrence of groundwater in the granitic aquifers.

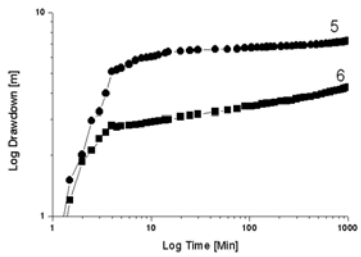

Figure 9. Pumping test results of wells 5 and 6, see fig. 3b for location.

4 CONCLUSIONS

Digital analysis of remote sensing data using different methods has permitted identification of various rock types and major lineaments. The satellite interpretations form an excellent basis for a GIS, which is ideal as a tool for groundwater potential assessment. The use of a GIS is a very time- and cost-effective approach once the database is created and has many advantages over traditional approaches. However, to fully understand the hydrogeological nature of hard rock aquifers, the traditional approach is also crucial. In this study field investigations allowed to understand the nature of lineaments as well as the hydrogeological setting. High yielding wells and springs are often related to large lineaments and corresponding structural features. The N-S oriented fractures appear to be associated with the high yielding wells and can be used as primary targets for groundwater exploration. Fractures in hydraulic connection with alluvium and weathered bedrock constitute best aquifers. The overall results demonstrate that the integration of remote sensing, GIS and traditional fieldwork provide a powerful tool in the assessment of water resources.

ACKNOWLEDGEMENT

This study is supported financially by SIDA /SAREC as part of a cooperation between Uppsala University, Sweden and the University of Asmara (UoA), Eritrea. Special thanks go to the Water Resources Department (WRD) in Eritrea for providing all types of data and Dr. S. Drury for facilitating the availability of the Landsat TM data. We want to extend our thanks to Mr. G.M. Hagos (Head WRD), Mr. M. Negash (Head Groundwater Division in WRD), Dr. Y. Zecarias (Head ERIWESP project in WRD), Mr. T. Yemane, Mr. S. Berhe, Mr. Asmelash, Mrs. Freweini and all staff members of the WRD. Thanks are due to Drs. M. Teklay, W. Ghebreab and B. W/Haimanot (UoA), for their encouragement to carry out this work. Fieldwork assistance and discussions with Mr. T. Zerai (UWRC) was highly appreciated. The authors are grateful to Dr. S.M. Berhe (African Resources Co.) Mr. E. Asrat (GEDDEC), Mr. K. Tsige, Mr. S. Foto and Mr. Mesghina (MoLG), and Mr K. Tesfai (ECDC) for their unlimited assistance in providing additional data.

REFERENCES

Drury, S.A., 1987. Image Interpretation in Geology (London: Allen & Unwin), 243 pp.

Drury, S.A., & Berhe, S.M., 1993. Accretion tectonics in northern Eritrea revealed by remotely sensed imagery. Geol. Mag., 130 (2), pp 170-190.

Ghebreab, W. 1996. An outline of major Pan-African lithologic assemblages and shear zones in Eritrea: implications for mineral exploration. African Geoscience Review, 3, pp. 355 - 366.

Jensen, J.R., 1986. Introductory Digital Image Processing: A Remote Sensing Perspective (Englewood Cliffs, New Jersey: Prentice-Hall), 379 pp.

Krishnamurthy, J.,Kumar, N.V., Jayaraman, V., and Manivel, M., 1996. An approach to demarcate groundwater potential zones through remote sensing and a geographic information system. Int. J. Remote Sensing, 17, pp. 1867-1884.

Lillesand, T.M., and Kiefer, R.W., 1994. Remote Sensing and Image Interpretation (Newyork: Wiley), 750 pp.

Sabins, F.F., 1978. Remote Sensing Principles and Interpretation. (San Francisco, Calif. : W.H. Freeman), 449 pp.

Sander, P. 1996. Remote Sensing and GIS for Groundwater Assessment in Hard Rock Areas: Applications to water well siting in Ghana and Botswana. Chalmers Univ., Sweden. Publ A 80 Ph.D. dissertation.

Saraf, A.K. and Choudhury, P.R., 1998. Integrated remote sensing and GIS for Groundwater exploration and identification of Artificial recharge sites. Int. J. Remote Sensing, 19, pp. 1825-1841.

Sheffield, C., 1985. Selecting band combinations from multispectral data. Photogrammetric Engin. & Remote Sensing, 51, pp. 681-687.

Vail, J.R., 1987. Late Proterozoic terrains in the Arabian-Nubian Shield and their Characteristic mineralization. Geol. Jour., 22, pp. 161-174.